

## Photoelectron Spectroscopy of the Allyl and 2-Methylallyl Anions

Paul G. Wenthold, Mark L. Polak,<sup>†</sup> and W. C. Lineberger\*

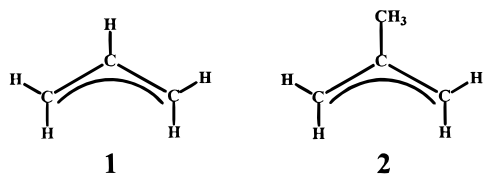
JILA, University of Colorado and National Institute of Standards and Technology and Department of Chemistry and Biochemistry, University of Colorado, Boulder, Colorado 80309-0440

Received: November 20, 1995; In Final Form: February 5, 1996<sup>⊗</sup>

The electron affinities of allyl, allyl-*d*<sub>5</sub>, 2-methylallyl, and 2-methylallyl-*d*<sub>7</sub> radicals have been determined from the 351 nm photoelectron spectra of the allylic anions. The ions were prepared in a cooled helium flow reactor by the reaction of O<sup>-</sup> with the corresponding propene. The electron affinities found for the radicals listed above are 0.481 ± 0.008, 0.464 ± 0.006, 0.505 ± 0.006, and 0.493 ± 0.008 eV, respectively. Extensive vibrational structure is observed in all the spectra, as the CCC bending and symmetric stretching modes are activated upon photodetachment. Vibrational frequencies for these modes are obtained for all of the radicals. A second harmonic of an asymmetric CH<sub>2</sub> rocking mode is observed in the spectra of the allyl, allyl-*d*<sub>5</sub>, and 2-methylallyl anions. Hot bands are used to determine the CCC bending frequencies in the allylic anions. Photoelectron angular distributions were measured for the allyl and 2-methylallyl anions. The photoelectron spectrum of allyl anion is calculated using a modeling procedure that utilizes the vibrational frequencies and geometries from *ab initio* calculations. This spectrum agrees very well with that obtained experimentally. The measured electron affinities are used together with the previously reported gas-phase acidities of propene and 2-methylpropene to determine the 298 K allylic C–H bond enthalpies for these hydrocarbons, with DH<sub>298</sub>(CH<sub>2</sub>CHCH<sub>2</sub>–H) = 88.8 ± 0.4 kcal/mol and DH<sub>298</sub>(CH<sub>2</sub>C(CH<sub>3</sub>)CH<sub>2</sub>–H) = 88.3 ± 2.3 kcal/mol. Methyl substitution at the 2-position of allyl radical is found to have little effect on any of the properties determined in this study.

### Introduction

Allyl radical, **1**, is among the most important and well-studied intermediates in all of chemistry. This species has been long recognized to possess special stability, which has been attributed to resonance stabilization, and the allyl radical is commonly used in studies of resonance in organic chemistry. Considering the long-standing interest in the allyl radical, it is not surprising that many studies of its physical properties have been carried out. Among the most informative is the EPR study by Fessenden and Schuler over 30 years ago,<sup>1</sup> where it was established that the allyl radical has C<sub>2v</sub> symmetry and negative spin density on the central carbon. This consequence of spin polarization in the radical was predicted by electronic structure calculations 5 years prior to the EPR experiments.<sup>2</sup>



The allyl radical has been studied using many experimental approaches. Along with the EPR studies,<sup>1,3</sup> there have been studies of the UV/vis absorption spectrum,<sup>4–7</sup> the IR spectrum in a matrix<sup>8–11</sup> and in the gas phase,<sup>12</sup> and the Raman spectrum.<sup>13–17</sup> A vibrational force field analysis for the radical and the deuterated isotopomer, **1D**, has been provided by Liu *et al.*<sup>17</sup> Additional spectroscopic information has come from multiphoton ionization studies.<sup>18–21</sup> The geometry of allyl radical was originally determined using electron diffraction,<sup>22</sup> but recently a more accurate experimental geometry has been obtained from the measured rotational constants for the C<sub>2v</sub>

molecule.<sup>12</sup> The structure and vibrational frequencies have been calculated using multiconfigurational Hartree–Fock (MCHF)<sup>23</sup> and multireference configuration interaction (MR-CI)<sup>24</sup> calculations as well as density functional theory (NLSD).<sup>25</sup>

The thermochemical properties of allyl radical have also been examined extensively. Many of these studies have been motivated by the desire to obtain a thermochemical estimate of the resonance stabilization in the allyl radical, cation and anion.<sup>26</sup> The ionization potential of allyl radical has been found to be 8.13 eV using photoelectron spectroscopy.<sup>27</sup> The electron affinity (EA) of allyl radical has also been reported previously. Brauman and co-workers obtained a value of 0.55 eV using infrared multiphoton photodetachment (IR photodetachment) of the allyl anion.<sup>28</sup> A lower value of 0.362 ± 0.020 eV was obtained by Oakes and Ellison<sup>29</sup> using photoelectron spectroscopy (PES) of the anion. In this paper, we report an improved photoelectron spectrum of allyl anion. Our spectrum is significantly better resolved than that previously reported, and we are able to detect extensive vibrational structure. A variable temperature ion source allows unequivocal assignment of the band origin. We show that the EA reported by Oakes and Ellison<sup>29</sup> is too low by approximately 0.1 eV. The EA of allyl radical is used in conjunction with the recently determined gas phase acidity of propene<sup>26</sup> to calculate the C–H bond enthalpy of propene. We have also measured the photoelectron spectra for the allyl-*d*<sub>5</sub>, 2-methylallyl, and 2-methylallyl-*d*<sub>7</sub> anions. These spectra provide electron affinities and spectroscopic information for the corresponding radicals.

### Experimental Section

The negative ion photoelectron spectrometer and experimental procedures have been described in detail previously,<sup>30,31</sup> and only a brief description is provided here. The ion source is a flowing afterglow, in which ions are created in a He buffer gas at a pressure of 0.4–0.7 Torr. Primary ions are created by

<sup>†</sup> Current address: Aerospace, Corp., El Segundo, CA.

<sup>⊗</sup> Abstract published in *Advance ACS Abstracts*, April 1, 1996.

seeding a small amount of source gas in a microwave discharge. For these studies, the primary reactant ion was the oxygen atomic anion,  $O^-$ , prepared from oxygen. The allyl anions required for this work were prepared by allowing the  $O^-$  to react with the corresponding propene introduced 10–30 cm downstream from the ion source. Because deprotonation of propene by  $O^-$  is endothermic by *ca.* 8 kcal/mol,<sup>32</sup> it is likely that the allyl ions are formed by  $OH^-$  ( $OD^-$ ) ions that are the result of a hydrogen (deuterium) transfer reaction between  $O^-$  and the corresponding propene.<sup>33</sup> Ions prepared in the flowing afterglow source are thermalized by collisions with the helium buffer gas. Liquid nitrogen is passed through a stainless steel jacket around the flowing afterglow in order to cool the ions.<sup>34</sup> Temperatures of the ions formed under these conditions are estimated to be *ca.* 185 K, based on the intensities of the hot bands in the photoelectron spectra (*vide infra*). Ions are gently extracted from the flowing afterglow through a 1 mm orifice into a differentially pumped region where they are accelerated, focused, mass-selected using a Wien velocity filter ( $M/\Delta M \approx 40$ ), and decelerated to 40 eV before they enter the laser interaction region.

The ion beam is crossed with the 351 nm output of an argon ion laser that has been injected into a buildup cavity encompassing the UV beam, using a previously described method.<sup>30</sup> The laser power within the cavity is estimated to be 30–50 W. The kinetic energies of the detached electrons are measured with a hemispherical electrostatic energy analyzer, with a resolution of 7–10 meV. The photoelectrons are detected using position-sensitive detection.<sup>30</sup>

The photoelectron spectrum depicts the number of photoelectrons, integrated over many scans, versus the electron kinetic energy (eKE). The absolute energy scale is calibrated using the  ${}^3P_2 + e^- \leftarrow {}^2P_{3/2}$  peak in the spectrum of  $O^-$  ( $EA(O) = 1.46112$  eV).<sup>35</sup> A small electron energy compression factor,  $\gamma$ , is determined by comparing measured fine structure peak positions with the known<sup>36</sup> term energies in the tungsten atom. The energy scale compression is on the order of 0.2%. The electron binding energy (eBE) is obtained by subtracting the electron kinetic energy from the laser photon energy, 3.531 19 eV.

**Materials.** All reagents were obtained from commercial suppliers and used as received. Propene (99%) and 2-methylpropene (99%) were obtained from Linde Specialty Gases and Matheson, respectively. Propene- $d_6$  (98%) was purchased from CIL, Inc., and 2-methylpropene- $d_8$  (99%) was obtained from C/D/N Isotopes. Additional gas purities were as follows: He, 99.995%;  $O_2$ , 99%.

## Results and Discussion

In this section, we report the photoelectron spectra for the allyl, allyl- $d_5$ , 2-methylallyl, and 2-methylallyl- $d_7$  anions. First, we describe the features that are observed in the spectra and provide comparisons with previous results reported in the literature. We report the results of Franck–Condon fits to the photoelectron spectra and show that the results for the allyl anion are similar to those obtained using an approach that utilizes the geometries and frequencies from *ab initio* calculations. Finally, we use the thermochemical properties obtained in this study to derive bond energies for propene and 2-methylpropene.

**Allyl and Allyl- $d_5$ .** The photoelectron spectra of the allyl anion,  $1^-$ , and the allyl- $d_5$  anion,  $1D^-$ , are shown in Figure 1 and Figure 2, respectively. As will be the case with all the spectra reported here, these data were collected utilizing ions formed in the liquid nitrogen cooled flowing afterglow. The origins of the observed band are found to be at  $3.051 \pm 0.008$

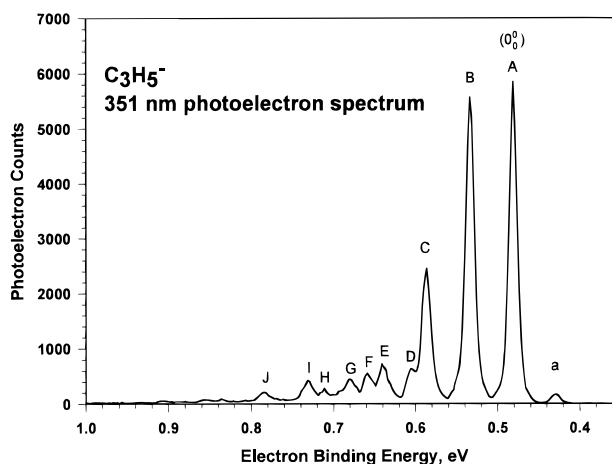


**Figure 1.** The 351 nm photoelectron spectrum of allyl anion,  $1^-$ . Positions and assignments of labeled peaks are provided in Table 2.

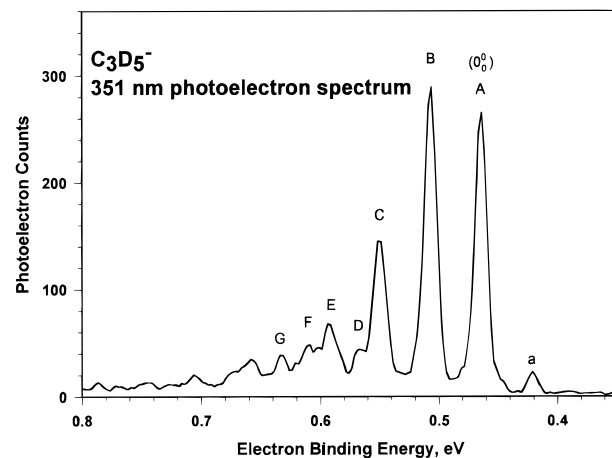


**Figure 2.** The 351 nm photoelectron spectrum of deuterated allyl anion,  $1D^-$ . Positions and assignments of labeled peaks are provided in Table 2.

and  $3.067 \pm 0.006$  eV (eKE) for  $1^-$  and  $1D^-$ , respectively. These values can be used to calculate  $EA(1) = 0.481 \pm 0.008$  eV and  $EA(1D) = 0.464 \pm 0.006$  eV. The electron affinities for all the systems examined in this study are listed in the top row of Table 1.

The spectra in Figures 1 and 2 are dominated by a single vibrational progression, peaks A, B, C, and E, with peak spacings of  $425$   $cm^{-1}$  in the spectrum of  $1^-$  and  $345$   $cm^{-1}$  in the spectrum of  $1D^-$ . The vibrational progressions observed in photoelectron spectra correspond to vibrations in the neutral that are activated upon detachment of an ion with a different geometry. Selection rules require that only totally symmetric modes are active. However, even harmonics of asymmetric modes are observed as well. The dominant mode observed in the spectra of  $1^-$  and  $1D^-$  is  $\nu_7$ , the CCC bending mode in the allyl radicals.<sup>17</sup> The values obtained here are in excellent agreement with the values of  $427$  and  $350$   $cm^{-1}$  recommended by Liu *et al.*,<sup>17</sup> based on Raman and IR spectroscopy results.<sup>13–17</sup> Oakes and Ellison<sup>29</sup> obtained values of  $395$  and  $380$   $cm^{-1}$  for these vibrational frequencies from their photoelectron spectra of the allyl and deuterated allyl anions, respectively.

Two additional weaker modes are observed in these spectra. In the spectrum of  $1^-$ , shown in Figure 1, the two frequencies are found to be  $990$  and  $1600$   $cm^{-1}$ . The  $990$   $cm^{-1}$  vibrational mode (peak D) most likely corresponds to  $\nu_6$  of allyl radical, a mixture of symmetric CCC stretching motion,  $CH_2$  scissoring, and  $CH_2$  rocking.<sup>17</sup> This mode has previously been assigned to be  $1068$   $cm^{-1}$  by Liu *et al.*<sup>17</sup> on the basis of the results of

**TABLE 1: Experimentally Determined Quantities from This Work**

R	allyl	allyl- <i>d</i> <sub>5</sub>	2-methylallyl	2-methylallyl- <i>d</i> <sub>7</sub>
EA(R), eV	0.481 ± 0.008	0.464 ± 0.006	0.505 ± 0.006	0.493 ± 0.008
DH <sub>298</sub> (R-H), <sup>a</sup> kcal/mol	88.8 ± 0.4 <sup>b</sup>		88.3 ± 2.3	
ΔH <sub>f,298</sub> (R), <sup>c</sup> kcal/mol	42.5 ± 0.4		32.2 ± 2.3	
ion CCC bending frequencies, <sup>d</sup> cm <sup>-1</sup>	425	350	425	
neutral vibrational frequencies, <sup>e</sup> cm <sup>-1</sup> (Δ <i>Q</i> <sub><i>i</i></sub> ) <sup>f</sup>				
CCC bending	425 (0.386)	345 (0.456)	430 (0.418)	350 (0.487)
CCC stretch	990 (0.092)	835 (0.124)	1030 (0.091)	845 (0.136)
CH <sub>2</sub> out-of-plane bending	1600 (0.061) <sup>g</sup>	1355 (0.070) <sup>g</sup>	1560(0.062) <sup>g</sup>	

<sup>a</sup> Calculated using eq 3. <sup>b</sup> This value contains a 0.2 ± 0.2 kcal/mol correction to convert EA(**1**) to the 298 K electron binding enthalpy. <sup>c</sup> Calculated using eq 4. <sup>d</sup> Determined from peak positions of hot bands; see Tables 2 and 3. Estimated uncertainty is ±20 cm<sup>-1</sup>. <sup>e</sup> Determined from average peak spacings; see Tables 2 and 3. Estimated uncertainty is ±20 cm<sup>-1</sup>. <sup>f</sup> Normal coordinate displacement in units of amu<sup>1/2</sup> Å. <sup>g</sup> Corresponds to *V* = 2 in this mode.

resonant Raman spectroscopy studies.<sup>14</sup> Values of 1242 and 972.8 cm<sup>-1</sup> have also been assigned to this mode on the basis of matrix IR spectra.<sup>8,10</sup> Theoretical predictions of this frequency range from 1018 to 1093 cm<sup>-1</sup> (unscaled values).<sup>23–25</sup> Scaling these values by a factor of 0.9 gives frequencies (920–985 cm<sup>-1</sup>) in fair agreement with that observed in the photoelectron spectrum. In the spectrum of **1D**<sup>-</sup>, the frequency of this transition is 835 cm<sup>-1</sup>. The difference between these frequencies in **1** and **1D** is in excellent agreement with that predicted by the MCHF calculations for the symmetric CCC stretching mode.<sup>23</sup> Getty and co-workers<sup>17</sup> have assigned a value 843 cm<sup>-1</sup> to  $\nu_4$  in C<sub>3</sub>D<sub>5</sub>. This mode consists mainly of CD<sub>2</sub> scissoring motion but also has contributions from CD<sub>2</sub> rocking and CCC stretching.

The weak transition at 1600 cm<sup>-1</sup> (peak G) in the photoelectron spectrum of **1**<sup>-</sup> does not correspond to any known vibrational mode in allyl radical and is most likely an overtone of  $\nu_{11}$ , the CH<sub>2</sub> out-of-plane bending mode.<sup>17</sup> A peak at 1600 cm<sup>-1</sup> was also observed in the matrix IR spectrum of allyl radical,<sup>10</sup> and was similarly assigned. The  $\nu_{11}$  fundamental is the most intense peak in the IR spectrum of the allyl radical,<sup>8–11</sup> with a vibrational frequency of 801 cm<sup>-1</sup>. It is possible that the observed transition at 1600 cm<sup>-1</sup> corresponds to the a<sub>2</sub> CH<sub>2</sub> out-of-plane bending mode,  $\nu_8$ , which has a value of 738 cm<sup>-1</sup>.<sup>10</sup> However, the results for the deuterated isomer described below rule out this assignment.

In the photoelectron spectrum of **1D**<sup>-</sup>, a transition is found at 1355 cm<sup>-1</sup>. Again, this does not correspond to any known frequencies of allyl-*d*<sub>5</sub><sup>17</sup> and is assigned to an overtone of  $\nu_{11}$ . Mal'tsev and co-workers<sup>10</sup> have reported a value of 640 cm<sup>-1</sup> for  $\nu_{11}$  in **1D**. From our spectrum, we estimate a value of 680 cm<sup>-1</sup>. The value for  $\nu_8$  in **1D** is predicted to be affected to an even greater extent in the deuterated molecule than is  $\nu_{11}$ . Liu *et al.*<sup>17</sup> assigned a value of 588 cm<sup>-1</sup> to  $\nu_8$  in **1D**. The overtone of this mode would be at *ca.* 1175 cm<sup>-1</sup>, 180 cm<sup>-1</sup> lower in energy than the peak in the photoelectron spectrum.

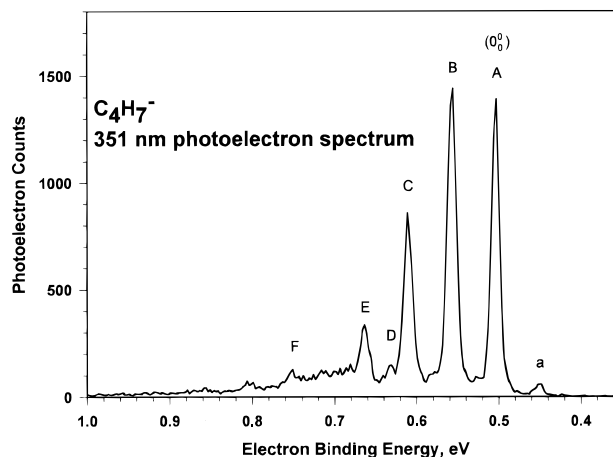
In addition to the features mentioned above, we observe hot bands in the photoelectron spectra of the allyl and allyl-*d*<sub>5</sub> anions, which result from detachment from a vibrationally excited state of the anion to the ground state of the radical. These peaks are 425 and 350 cm<sup>-1</sup> from the origin in the spectra of **1**<sup>-</sup> and **1D**<sup>-</sup>, respectively. These frequencies correspond to the CCC bending modes in the corresponding allyl anions. A complete listing of the energies of the observed peaks in Figures 1 and 2 is given in Table 2, along with the mode assignments.

**2-Methylallyl and 2-Methylallyl-*d*<sub>7</sub>.** The photoelectron spectra of the 2-methylallyl, **2**<sup>-</sup>, and deuterated 2-methylallyl, **2D**<sup>-</sup>, anions are shown in Figures 3 and 4, respectively. These spectra are qualitatively and quantitatively similar to those for **1**<sup>-</sup> and **1D**<sup>-</sup> shown in Figures 1 and 2, respectively. As before, the photoelectron spectra of **2**<sup>-</sup> and **2D**<sup>-</sup> are dominated by a

**TABLE 2: Peak Positions and Assignments for Photoelectron Spectra of **1**<sup>-</sup> and **1D**<sup>-</sup>**

peak <sup>a</sup>	allyl		allyl- <i>d</i> <sub>5</sub>	
	distance from origin, cm <sup>-1</sup>	assignment <sup>b</sup>	distance from origin, cm <sup>-1</sup>	assignment <sup>b</sup>
a	425	7 <sub>1</sub> <sup>0</sup>	350	7 <sub>1</sub> <sup>0</sup>
A	0	0 <sub>0</sub> <sup>0</sup>	0	0 <sub>0</sub> <sup>0</sup>
B	425	7 <sub>0</sub> <sup>1</sup>	345	7 <sub>0</sub> <sup>1</sup>
C	855	7 <sub>0</sub> <sup>2</sup>	690	7 <sub>0</sub> <sup>2</sup>
D	990	6 <sub>0</sub> <sup>1</sup>	835	4 <sub>0</sub> <sup>1</sup>
E	1270	7 <sub>0</sub> <sup>3</sup>	1035	7 <sub>0</sub> <sup>3</sup>
F	1415	6 <sub>0</sub> <sup>1</sup> 7 <sub>1</sub> <sup>0</sup>	1185	4 <sub>0</sub> <sup>1</sup> 7 <sub>1</sub> <sup>0</sup>
G	1600	11 <sub>0</sub> <sup>2</sup>	1355	11 <sub>0</sub> <sup>2</sup>
H	1855	6 <sub>0</sub> <sup>1</sup> 7 <sub>0</sub> <sup>2</sup>		
I	2020	11 <sub>0</sub> <sup>2</sup> 7 <sub>0</sub> <sup>1</sup>		
J	2445	11 <sub>0</sub> <sup>2</sup> 7 <sub>0</sub> <sup>2</sup>		

<sup>a</sup> Peaks labeled in Figures 1 (allyl) and 2 (allyl-*d*<sub>5</sub>). <sup>b</sup> See ref 17 for description of the normal modes.

**Figure 3.** The 351 nm photoelectron spectrum of 2-methylallyl anion, **2**<sup>-</sup>. Positions and assignments of labeled peaks are provided in Table 3.

vibrational progression corresponding to activation of the CCC bending mode of the allylic portion of the radical. In the 2-methylallyl radical, **2**, this mode has a frequency of 430 cm<sup>-1</sup>, while 350 cm<sup>-1</sup> is found for the same mode in the deuterated isomer, **2D**. The origins of the bands are at 3.026 ± 0.006 and 3.038 ± 0.008 eV (eKE) for Figures 3 and 4, respectively, giving EA(**2**) = 0.505 ± 0.006 and EA(**2D**) = 0.493 ± 0.008 eV (Table 1). From the hot band evident in Figure 3, we obtain a value of 430 cm<sup>-1</sup> for the CCC bending mode in **2**<sup>-</sup>.

The symmetric CCC stretching modes in the allyl and allyl-*d*<sub>5</sub> radicals that were active in the spectra of **1**<sup>-</sup> and **1D**<sup>-</sup> are also observed in the spectra of the 2-methylallyl anions. For **2**, this mode is found to be 1030 cm<sup>-1</sup> while a value of 845 cm<sup>-1</sup> is obtained for the CCC stretching mode of **2D**. These

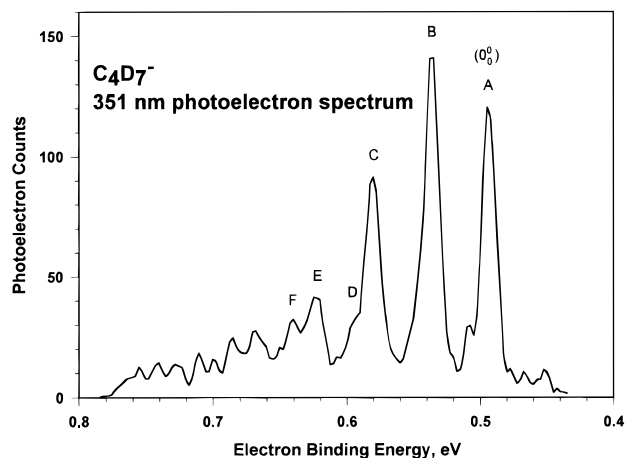


**Figure 4.** The 351 nm photoelectron spectrum of deuterated 2-methylallyl anion,  $2\mathbf{D}^-$ . Positions and assignments of labeled peaks are provided in Table 3.

**TABLE 3: Peak Positions and Assignments for Photoelectron Spectra of  $2^-$  and  $2\mathbf{D}^-$**

peak <sup>a</sup>	2-methylallyl		2-methylallyl- <i>d</i> <sub>7</sub>	
	distance from origin, cm <sup>-1</sup>	assign <sup>b</sup>	distance from origin, cm <sup>-1</sup>	assign <sup>b</sup>
a	425	1 <sub>1</sub> <sup>0</sup>		
A	0	0 <sub>0</sub> <sup>0</sup>	0	0 <sub>0</sub> <sup>0</sup>
B	430	1 <sub>0</sub> <sup>0</sup>	345	1 <sub>0</sub> <sup>1</sup>
C	860	1 <sub>0</sub> <sup>2</sup>	705	1 <sub>0</sub> <sup>2</sup>
D	1030	2 <sub>0</sub> <sup>1</sup>	845	2 <sub>0</sub> <sup>1</sup>
E	1290	1 <sub>3</sub> <sup>3</sup>	1050	1 <sub>0</sub> <sup>3</sup>
F	1990	1 <sub>0</sub> 3 <sub>0</sub> <sup>2</sup>	1190	1 <sub>0</sub> 2 <sub>0</sub> <sup>1</sup>

<sup>a</sup> Peaks labeled in Figures 3 (2-methylallyl) and 4 (2-methylallyl-*d*<sub>7</sub>). <sup>b</sup> Vibrational mode assignments are as follows: 1, CCC bending; 2, symmetric CC stretching; 3, CH<sub>2</sub> out-of-plane bending.

correspond well with what were found for **1** and **1D**. The transition corresponding to the second harmonic of the CH<sub>2</sub> out-of plane bending mode observed in the spectra of the allyl and allyl-*d*<sub>5</sub> anions is found to be 1560 cm<sup>-1</sup> in the spectrum of  $2^-$ . It could not be determined from the spectrum of  $2\mathbf{D}^-$  because of a lower signal-to-noise ratio, principally a consequence of a limited supply of expensive deuterated 2-methylpropene (\$900/liter).

The measured vibrational frequencies for **2** can be compared to those observed in the IR spectrum of matrix-isolated 2-methylallyl radical reported by Avakyan *et al.*<sup>37</sup> The most intense band in the IR spectrum is the CH<sub>2</sub> rocking mode, at 795 cm<sup>-1</sup>. The peak at 1560 cm<sup>-1</sup> in the photoelectron spectrum of 2-methylallyl anion agrees well with what would be expected for twice this mode. Avakyan *et al.* predicted that methyl substitution should have a significant effect on the CCC bending mode of the allyl radical based on UHF calculations with small basis sets.<sup>37</sup> This aspect is not supported by our data, as the CCC bending frequencies obtained for radicals **1** and **2** are essentially indistinguishable. The positions and vibrational assignments for the peaks marked in Figures 3 and 4 are listed in Table 3.

**Angular Distribution Measurements.** The angular distribution of the average photoelectron signal is described by eq 1, where  $\theta$  is the angle between the laser electric field and the electron detector and  $\beta$  is the anisotropy parameter ( $-1 \leq \beta \leq 2$ ).

$$I(\theta) = (I_{\text{av}}/4\pi)(1 + \beta(3 \cos^2 \theta - 1)/2) \quad (1)$$

The previous spectra were all measured with the laser electric field polarized at 54.7° (the “magic angle”), where  $I(\theta) = I_{\text{av}}$ . Photoelectron spectra for  $1^-$  and  $2^-$  were also measured with laser polarizations of 0° and 90°. Cooper and Zare have demonstrated that the anisotropy parameter for electron detachment,  $\beta$ , can be estimated from the photodetachment yields for these conditions using the relationship shown in eq 2,<sup>38,39</sup> where  $I_0$  and  $I_{90}$  are the photoelectron yields at laser polarizations of 0° and 90°, respectively.

$$\beta = (I_0 - I_{90})/(0.5I_0 + I_{90}) \quad (2)$$

The anisotropy parameters obtained for photodetachment from the allyl and 2-methylallyl anions are  $-0.60$  and  $-0.57$ , respectively. These values are similar in sign and magnitude to those reported previously for the benzyl and phenoxide anions,<sup>40</sup>  $-0.42$  and  $-0.53$ , respectively, and are consistent with what is expected for detachment for allylic systems where the electron is in a p-like ( $\pi$ ) orbital. Although angular distributions were not measured for the perdeuterio anions, they are expected to be comparable to those obtained for the undeuterated ions.

**Franck–Condon Fitting and Modeling of Photoelectron Spectra.** The analysis of the photoelectron spectrum begins with the recognition of sequences of transitions corresponding to various quanta of a given vibrational normal mode. The relative intensities of these transitions depend upon the geometry difference between the anion and the neutral in a given normal coordinate. In general, the vibrational intensities in the photoelectron spectra can be accurately reproduced using a Franck–Condon fitting procedure described elsewhere.<sup>30</sup> The Franck–Condon factors determined from such a fit are essentially the “normal-coordinate displacements”,  $\Delta Q_i$ , the elements of the Duschinsky **K** matrix,<sup>41</sup> and reflect the geometry differences within each normal coordinate between the ion and the neutral. Franck–Condon factors are obtained from the photoelectron spectrum using an iterative nonlinear least-squares procedure in which the Franck–Condon factor for each vibrational mode is optimized in order to minimize the deviation between the calculated and experimental spectrum.<sup>30</sup> Since the electron affinity, origin peak height, peak widths, and vibrational frequencies can be determined directly from the spectrum, the only adjustable parameters in the fitting procedure are the normal-coordinate displacements.<sup>42</sup> The active vibrational modes and the optimized Franck–Condon factors for photodetachment for all the systems examined here are listed in at the bottom of Table 1. Not surprisingly, the Franck–Condon factors for comparable modes are similar for all the ions. This is consistent with what is expected qualitatively based on the similar appearance of all the photoelectron spectra.

The Franck–Condon factors can also be calculated directly if the geometries and force fields for the ions and neutrals are known. Unfortunately, this information is rarely available for ions and radicals. However, *ab initio* calculations can be used to calculate accurate geometries and frequencies for these molecules. These parameters are generally much better determined than are the total or relative energies for the states. Chen and co-workers<sup>43</sup> have recently developed a software suite that calculates the Duschinsky **K** matrix directly using the reduced-mass-weighted atom displacements that are generated in a GAUSSIAN force constant calculation.<sup>44</sup> The calculated vibrational frequencies and Franck–Condon factors can be compared directly to those obtained using the fitting procedure described above, or they can be used along with the experimental electron affinity and peak widths to calculate the photoelectron spectrum using a method described previously.<sup>30,45</sup> In this case, the only adjustable parameters are the electron affinity, origin

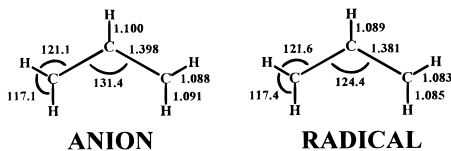


**Figure 5.** Geometries of the allyl anion,  $1^-$ , and the allyl radical,  $1$ , optimized at the MP2/6-31+G\* level of theory.

**TABLE 4: Vibrational Modes and Franck–Condon Factors Obtained from Empirical Modeling of the Photoelectron Spectrum of  $1^-$**

vib mode, <sup>a</sup> cm <sup>-1</sup>	$\Delta Q_i$ , amu <sup>1/2</sup> Å	vib mode, <sup>a</sup> cm <sup>-1</sup>	$\Delta Q_i$ , amu <sup>1/2</sup> Å
405	-0.387	2940	0.007
985	-0.108	2950	0.014
1220	-0.004	3040	0.002
1440	-0.012		

<sup>a</sup> Frequencies calculated at the MP2/6-31+G\* level of theory, scaled by 0.91.

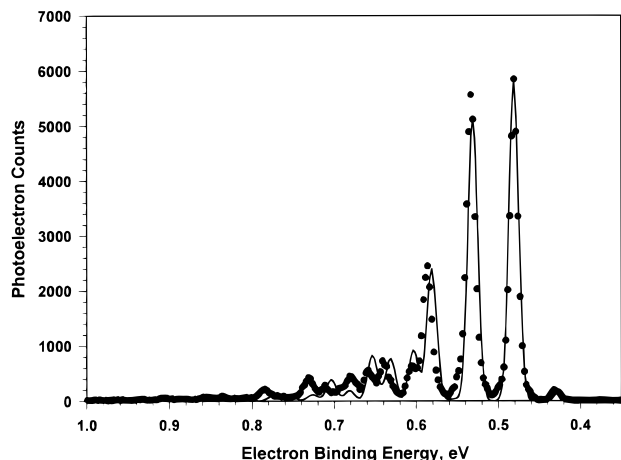


**Figure 6.** Experimental (●) and simulated (solid line) photoelectron spectrum of allyl anion. See text for details.

peak height, and peak width, and these are set so they match the experimental results.

As an example, we have calculated the photoelectron spectrum of the allyl anion. The geometries and frequencies for the allyl radical and anions were calculated at the MP2/6-31+G\* level of theory.<sup>46</sup> The optimized geometries for these species are shown in Figure 5. The active vibrational modes corresponding to Franck–Condon factors calculated for these geometries are listed in Table 4. These can be compared with the parameters obtained by fitting the experimental data listed at the bottom of the first column in Table 3. The calculated vibrational frequencies (scaled by a factor of 0.91) and Franck–Condon factors for the CCC bending and symmetric stretching modes obtained from the simulation are in excellent agreement with those obtained from fitting the spectrum. Moreover, five additional modes are predicted to be active in the photodetachment of allyl anion. However, the Franck–Condon factors for these modes are all too small to produce observable peaks in the photoelectron spectra. The simulated photoelectron spectrum, calculated using the parameters listed in Table 4 along with experimental values for the peak width and the spectrum origin peak energy and intensity, is shown as a solid line in Figure 6. The observed photoelectron spectrum of the allyl anion, indicated by black circles in Figure 6, is reproduced very well by the simulation, with the exception of the overtone at 1600 cm<sup>-1</sup>. However, this discrepancy arises because we have not included  $\Delta V = 2$  overtones of non-totally symmetric vibrations in the modeling procedures.

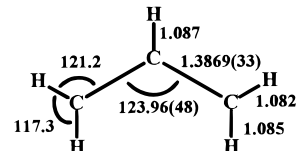
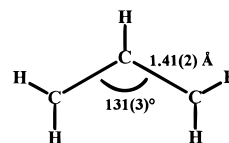


**Figure 7.** Experimentally determined structure of allyl radical (taken from ref 12).

The excellent agreement between the experimental and empirically determined Franck–Condon parameters suggests that the relative geometries of the allyl anion and allyl radical calculated at the MP2/6-31+G\* level of theory are sufficiently accurate for modeling the photoelectron spectrum. Thus, it is possible to use the calculated geometry differences along with the known structure of the allyl radical to determine the geometry of the allyl anion. The equilibrium geometry of allyl radical determined from the rotational constants<sup>12</sup> is shown in Figure 7. This geometry agrees very well with that calculated at the MP2/6-31+G\* level of theory, shown in Figure 5. The relative bond lengths calculated for the allyl radical and allyl anion (Figure 5) are reasonably accurate, as indicated by the excellent agreement between the calculated and experimental Franck–Condon factors. Therefore, the C–C bond length in the allyl anion is *ca.* 0.02 Å longer than that of the allyl radical,  $1.3869 \pm 0.0033$  Å.<sup>12</sup> Moreover, the CCC bond angle in the allyl anion is estimated to be 7° larger than the corresponding angle in the allyl radical,  $123.96 \pm 0.48^\circ$ , determined from the rotational constants.<sup>12</sup> On the basis of these comparisons, we arrive at the following structure for the allyl anion:



The remaining differences between the ion and the neutral are negligible.

**Thermochemical Properties.** The electron affinities of the allyl, allyl-*d*<sub>5</sub>, 2-methylallyl, and 2-methylallyl-*d*<sub>8</sub> radicals measured in this study are listed in the first row of Table 1. The electron affinity obtained for the allyl radical is similar to the value reported by Brauman and co-workers<sup>28</sup> but is significantly higher than that obtained by Oakes and Ellison (OE) using negative ion photoelectron spectroscopy.<sup>29</sup> However, this discrepancy is understood by recognizing that the OE experiments were carried out using a discharge ion source in which ions are formed with significant vibrational energies. The band assigned as the origin by Oakes and Ellison most likely corresponds to a transition from  $V = 2$  of the CCC bend in the anion to  $V = 0$  in the radical. This explanation also accounts for the discrepancy between our value for the EA of **1D** and the OE value. The electron affinities for **2** and **2D** are only slightly higher than the corresponding allyl radicals. This indicates that methyl substitution at the 2-position does not significantly stabilize the allyl anion.

The measured electron affinities for **1** and **2** can be used to derive the bond energies ( $DH_{298}(R-H)$ ) in propene and 2-methylpropene via the thermochemical cycle given by eq 3, where

$$DH_{298}(R-H) = EA(R) + \Delta H_{\text{acid}}(R-H) - IP(H) \quad (3)$$

$\Delta H_{\text{acid}}(RH)$  refers to the 298 K gas-phase acidity of propene or 2-methylpropene (isobutylene). In order to calculate the bond dissociation enthalpies using eq 3, it necessary to convert the measured, adiabatic electron affinity, a 0 K quantity, to the 298

K electron binding enthalpy.<sup>47</sup> This temperature correction amounts to the difference between the heat capacities of the anion and the radical integrated between 0 and 300 K. The correction is typically very small (<0.3 kcal/mol) and is neglected frequently because it is usually much smaller than the overall uncertainty.

The gas-phase acidities of propene<sup>26</sup> and 2-methylpropene<sup>32,48</sup> have been determined previously using forward and reverse proton transfer rate measurements to be  $391.1 \pm 0.3$  and  $390.3 \pm 2.3$  kcal/mol, respectively. The 298 K bond dissociation enthalpies for propene and 2-methylpropene derived with use of eq 3 are  $88.8 \pm 0.4$  and  $88.3 \pm 2.3$  kcal/mol, respectively (Table 1). The value given for propene includes a  $0.2 \pm 0.2$  kcal/mol temperature correction, calculated by Davico *et al.*,<sup>26</sup> in order to convert EA(1) to the 300 K electron binding enthalpy. The value reported for 2-methylpropene does not contain any temperature correction. The bond enthalpies for propene and 2-methylpropene can be used to calculate the heats of formation for the allyl and 2-methylallyl radicals according to equation 4.

$$\Delta H_{f,298}(\text{R}) = \text{DH}_{298}(\text{R-H}) + \Delta H_{f,298}(\text{RH}) - \Delta H_{f,298}(\text{H}) \quad (4)$$

The experimental heats of formation of propene and 2-methylpropene are  $4.8 \pm 0.2$  and  $-4.0 \pm 0.1$  kcal/mol, respectively,<sup>49</sup> and the 298 K heat of formation of the hydrogen atom is 52.1 kcal/mol.<sup>50</sup> Using these values and the bond enthalpies listed in Table 1, we obtain  $\Delta H_{f,298}(\mathbf{1}) = 41.5 \pm 0.4$  kcal/mol and  $\Delta H_{f,298}(\mathbf{2}) = 32.2 \pm 2.3$  kcal/mol. These quantities are also listed in Table 1.

The bond enthalpies and heats of formation determined in this study can be compared to what has been reported previously. McMillan and Golden<sup>51</sup> and Benson<sup>52</sup> recommend a value of  $\text{DH}_{300}(\text{CH}_2\text{CHCH}_2\text{-H}) = 87 \pm 1$  kcal/mol, in fair agreement with that obtained here. Golden and co-workers have reported values of  $\Delta H_{f,300}(\mathbf{1}) = 39.4 \pm 1.5$  and  $39.1 \pm 1.5$  kcal/mol based on halogen abstraction<sup>53</sup> and radical dimerization kinetics measurements,<sup>54,55</sup> respectively. Tsang and Walker<sup>56</sup> found  $\Delta H_{f,298}(\mathbf{1}) = 40.9 \pm 1.0$  kcal/mol from their shock tube studies of the decomposition of 1,7-octadiene. The bond enthalpy of propene and heat of formation of allyl radical determined here are consistent with the previous reported values but are more precise.

Lias and Ausloos<sup>57</sup> have estimated a value for the heat of formation of **2** from the proton affinity. Using proton transfer bracketing experiments, they determined that the proton affinity (PA) of **2** was between that of *p*-fluorotoluene and nitroethane and assigned a value of 185.3 kcal/mol. This value can be used together with the heat of formation of the isobutylene cation (209.1 kcal/mol) to obtain  $\Delta H_{f,298}(\mathbf{2}) = 28.7$  kcal/mol, which corresponds to  $\text{DH}_{298}(\text{CH}_2\text{C}(\text{CH}_3)\text{CH}_2\text{-H}) = 84.8$  kcal/mol. However, the proton affinity scale has undergone modification recently,<sup>58</sup> such that proton affinities of the reference molecules may be slightly lower than those used by Lias and Ausloos.<sup>57</sup> If this is the case, then the heat of formation of **2** would be slightly lower as well.

The significance of the bond enthalpy in propene in terms of the resonance energy in allyl has been discussed recently by Ellison and co-workers.<sup>26</sup> Briefly, the difference between the C-H bond enthalpy in propene and in a model hydrocarbon, such as propane, can be attributed to the resonance energy in

the allyl radical. Ellison and co-workers<sup>26</sup> calculate a value of 14 kcal/mol for this quantity, which compares favorably to most estimates of the resonance energy.

**Acknowledgment.** This work was supported by the National Science Foundation (Grants CHE 93-18639 and PHY 90-12244). We thank Mr. Cameron Logan for his assistance with the spectra modeling. We also thank Prof. Barney Ellison and Mr. Bob Gunion for stimulating discussion and assistance.

## References and Notes

- (1) Fessenden, R. W.; Schuler, R. H. *J. Chem. Phys.* **1968**, *39*, 2147.
- (2) McConnell, H. M.; Chestnut, D. B. *J. Phys. Chem.* **1958**, *28*, 107.
- (3) McManus, H. J.; Fessenden, R. W.; Chipman, D. M. *J. Phys. Chem.* **1988**, *92*, 3778.
- (4) Currie, C. L.; Ramsey, D. A. *J. Chem. Phys.* **1966**, *45*, 488.
- (5) Callear, A. B.; Lee, H. K. *Trans. Faraday Soc.* **1968**, *64*, 308.
- (6) Bergh, H. E. v. d.; Callear, A. B. *Trans. Faraday Soc.* **1970**, *66*, 2681.
- (7) Nakashima, N.; Yoshihara, K. *Laser Chem.* **1987**, *7*, 177.
- (8) Maier, G.; Reisenauer, H. P.; Rohde, B.; Dehnicke, K. *Chem. Ber.* **1983**, *116*, 732.
- (9) Mal'tsev, A. K.; Korolov, V. A.; Nefedov, O. M. *Izv. Akad. Nauk SSSR, Ser. Khim.* **1982**, 2415.
- (10) Mal'tsev, A. K.; Korolev, V. A.; Nefedov, O. M. *Izv. Akad. Nauk SSSR, Ser. Khim.* **1984**, 555.
- (11) Huang, J. W.; Graham, R. M. *J. Chem. Phys.* **1990**, *93*, 1583.
- (12) Hirota, E.; Yamada, C.; Okunishi, M. *J. Chem. Phys.* **1992**, *97*, 2963.
- (13) Getty, J. D.; Burmeister, M. J.; Westre, S. G.; Kelly, P. B. *J. Am. Chem. Soc.* **1991**, *113*, 801.
- (14) Getty, J. D.; Kelly, P. B. *Chem. Phys.* **1992**, *168*, 357.
- (15) Getty, J. D.; Liu, X.; Kelly, P. B. *J. Phys. Chem.* **1992**, *96*, 10155.
- (16) Getty, J. D.; Liu, X.; Kelly, P. B. *Chem. Phys. Lett.* **1993**, *201*, 236.
- (17) Liu, X.; Getty, J. D.; Kelly, P. B. *J. Chem. Phys.* **1993**, *99*, 1522.
- (18) Hudgens, J. W.; Dulcey, C. S. *J. Phys. Chem.* **1985**, *89*, 1505.
- (19) Sappy, A. D.; Weisshaar, J. C. *J. Phys. Chem.* **1987**, *91*, 3731.
- (20) Minsek, D. W.; Blush, J. A.; Chen, P. *J. Phys. Chem.* **1992**, *96*, 2025.
- (21) Blush, J. A.; Minsek, D. W.; Chen, P. *J. Phys. Chem.* **1992**, *96*, 10150.
- (22) Vajda, E.; Tremmel, J.; Rozsondai, B.; Hargittai, I.; Maltsev, A. K.; Kagramanov, N. D.; Nefedov, O. M. *J. Am. Chem. Soc.* **1986**, *108*, 4352.
- (23) Takada, T.; Dupois, M. *J. Am. Chem. Soc.* **1983**, *105*, 1713.
- (24) Szalay, P. G.; Császár, A. G.; Fogarasi, G.; Karpfen, A.; Lischka, H. *J. Chem. Phys.* **1990**, *93*, 1246.
- (25) Sim, F.; Salahub, D. R.; Chin, S.; Dupuis, M. *J. Chem. Phys.* **1991**, *95*, 4317.
- (26) Davico, G. E.; Bierbaum, V. M.; DePuy, C. H.; Ellison, G. B. *Int. J. Mass Spectrom. Ion Processes*, in press.
- (27) Houle, F. A.; Beauchamp, J. L. *J. Am. Chem. Soc.* **1978**, *100*, 3290.
- (28) Meyer, F. K.; Jasinski, J. M.; Rosenfeld, R. N.; Brauman, J. I. *J. Am. Chem. Soc.* **1982**, *104*, 663.
- (29) Oakes, J. M.; Ellison, G. B. *J. Am. Chem. Soc.* **1984**, *106*, 7734.
- (30) Ervin, K. M.; Lineberger, W. C. In *Gas Phase Ion Chemistry*; Adams, N. G., Babcock, L. M., Eds.; JAI Press: Greenwich, 1992; Vol. 1, p 121.
- (31) Leopold, D. G.; Murray, K. K.; Stevens-Miller, A. E.; Lineberger, W. C. *J. Chem. Phys.* **1985**, *83*, 4849.
- (32) Lias, S. G.; Bartmess, J. E.; Liebman, J. L.; Holmes, J. L.; Levin, R. D.; Mallard, W. G. *J. Phys. Chem. Ref. Data* **1988**, *17* (Suppl. 1).
- (33) Lee, J.; Grabowski, J. J. *Chem. Rev.* **1992**, *92*, 1611.
- (34) Robinson, M. S.; Polak, M. L.; Bierbaum, V. M.; DePuy, C. H.; Lineberger, W. C. *J. Am. Chem. Soc.* **1995**, *117*, 6766.
- (35) Neumark, D. M.; Lykke, K. R.; Andersen, T.; Lineberger, W. C. *Phys. Rev. A* **1985**, *32*, 1890.
- (36) Moore, C. E. *Atomic Energy Levels*; US GPO Circular No. 467; US GPO: Washington, DC, 1952.
- (37) Avakyan, V. G.; Volkova, V. V.; Gusel'nikov, L. E.; Ziegler, U.; Zimmerman, G.; Ondruschka, B.; Nametkin, N. S. *Dokl. Akad. Nauk SSSR* **1986**, *290*, 1133.
- (38) Cooper, J.; Zare, R. N. *J. Chem. Phys.* **1968**, *48*, 942.
- (39) Cooper, J.; Zare, R. N. *J. Chem. Phys.* **1968**, *49*, 4252.
- (40) Gunion, R. F.; Karney, W.; Wenthold, P. G.; Borden, W. T.; Lineberger, W. C. *J. Am. Chem. Soc.*, submitted.
- (41) Duschinsky, F. *Acta Physicochim. URSS* **1937**, *7*, 551.
- (42) If hot bands are included in the simulation, the temperature of the ion can be optimized simultaneously.

(43) Chen, P. In *Unimolecular and Bimolecular Reaction Dynamics*; Ng, C. Y., Baer, T., Powis, I., Eds.; John Wiley & Sons: New York, 1994.

(44) We thank Peter Chen and Cameron Logan for providing us with a copy of their CDECK program.

(45) Ervin, K. M.; Ho, J.; Lineberger, W. C. *J. Phys. Chem.* **1988**, *92*, 5405.

(46) Frisch, M. J.; Head-Gorden, M.; Trucks, G. W.; Gill, P. M.; Wong, M. W.; Foresman, J. B.; Johnson, B. G.; Schlegel, H. B.; Replogle, E. S.; Gomperts, R.; Andres, J. L.; Raghavachari, K.; Robb, M. A.; Binkley, J. S.; Gonzales, C.; Defrees, D. J.; Fox, D. J.; Baker, J.; Martin, R. L.; Pople, J. A. *GAUSSIAN92, Revision E*; Gaussian, Inc.: Pittsburgh, PA, 1992.

(47) Berkowitz, J.; Ellison, G. B.; Gutman, D. *J. Phys. Chem.* **1994**, *98*, 2744.

(48) Bartmess, J. E.; Burnham, R. D. *J. Org. Chem.* **1984**, *49*, 1382.

(49) Pedley, J. B.; Naylor, R. D.; Kirby, S. P. *Thermochemistry of Organic Compounds*, 2nd ed.; Chapman and Hall: New York, 1986.

(50) Chase Jr., M. W.; Davies, C. A.; Downey Jr., J. R.; Frurip, D. J.; McDonald, R. A.; Syverud, A. N. *J. Phys. Chem. Ref. Data* **1985**, *14*, Suppl. 1 (JANAF Tables).

(51) McMillan, D. F.; Golden, D. M. *Annu. Rev. Phys. Chem.* **1982**, *33*, 493.

(52) Benson, S. W. *Thermochemical Kinetics*, 2nd ed.; Wiley-Interscience: New York, 1976.

(53) Rossi, M.; Golden, D. M. *J. Am. Chem. Soc.* **1979**, *101*, 1230.

(54) Golden, D. M.; Benson, S. W. *J. Am. Chem. Soc.* **1969**, *91*, 2136.

(55) Rossi, M.; King, K. D.; Golden, D. M. *J. Am. Chem. Soc.* **1979**, *101*, 1223.

(56) Tsang, W.; Walker, J. A. *J. Phys. Chem.* **1992**, *96*, 8378.

(57) Lias, S. G.; Ausloos, P. *Int. J. Mass Spectrom. Ion Processes* **1987**, *81*, 165.

(58) Szulejko, J. E.; McMahon, T. B. *J. Am. Chem. Soc.* **1993**, *115*, 7839.

JP953401N